Hindawi
International Journal of Antennas and Propagation
Volume 2023, Article ID 3008738, 13 pages
https://doi.org/10.1155/2023/3008738

Research Article

A Multi-Polarized Reconfigurable Plasma Antenna Array

Zhen Sun, Zhenzhen Zhou, Zhihao Tan, Huafeng Wu, and Jiansen Zhao

Merchant Marine College, Shanghai Maritime University, Shanghai 201306, China

Correspondence should be addressed to Jiansen Zhao; jszhao@shmtu.edu.cn

Received 29 April 2023; Revised 8 July 2023; Accepted 9 August 2023; Published 11 September 2023

Academic Editor: Alessandro Di Carlofelice

Research on antenna reconfiguration is important in antenna applications. We present design of a multi-polarized plasma antenna with 40.68 MHz radio frequency (RF) power supplies and several discharge tubes filled with argon (neon) and mercury. Furthermore, self-made regulating circuits among the vibrators are introduced for the antenna array system. It can not only make the length of the dipole controllable but also improve the antenna gain and circular polarization (CP) performance under different lengths. Antenna arrays can be classified into linear and circular polarization by quickly adjusting the phase difference between vibrators. Both the experimental and simulation results indicate that the plasma antenna can realize impedance, pattern, and polarization reconstruction expediently. In addition, the linear polarization (LP) and CP can be transformed into each other quickly by adjusting the discharge conditions and regulating circuits. Moreover, compared with a symmetrical cross vibrator plasma antenna and a metal antenna of the same size, the proposed antenna array shows a certain gain and good reconfigurable performance within the frequency band of 150–250 MHz.

1. Introduction

For several years, the problem of plasma reconstruction of plasma antennas has been proposed [1, 2]. Plasma antenna is a type of radio frequency (RF) antenna for radiating and receiving electromagnetic (EM) waves under certain conditions. In other words, the metal elements of a conventional antenna can be replaced with plasma element medium. An antenna array can be established in the complex plasma antenna system. Plasma antennas offer some distinct advantages compared to conventional metallic antennas [3–6] like simple structure and rapid reconfiguration. Besides, in the plasma antenna array system, the mutual coupling effect between the vibrators is relatively low [7]. Simultaneously, plasma permits antenna structures to be reconfigurable concerning antenna shape, working frequency, signal bandwidth, pattern, polarization, directivity, and gain on millisecond to microsecond timescales [4, 8, 9]. For defense applications, plasma antenna presents stealth features by being quickly deionized when scanned by the radar detection device. Therefore, the plasma antenna or its array can be used for reconfigurable antenna, beamforming, military applications, etc.

Plasma antennas have attracted the attention of researchers because of their benefits, such as stealth and rapid reconstruction. Borg et al. [3] studied the properties like efficiencies and radiation patterns of the monopole antenna, which has been used in communication applications. Papadimopoulos and Di Iorio [7] tested the excitation of a plasma antenna using the argon surface wave discharge operating at 500 MHz with RF power levels up to 120 W. Kumar and Bora [10–12] showed that plasma shape in the discharge tube can be changed by modifying the plasma parameters, like linear, helix, and spiral. Ye et al. [13] have established the system equations of plasma linear antenna according to the rule of the disturbing current and further identified the noise. Russo et al. [14, 15] have studied the properties of the plasma column antenna in both qualitative and quantitative manner. Zhao et al. [16–19] studied the flexible plasma antenna and achieved the performance of regulating antenna pattern, gain, bandwidth, and even polarization by changing its shape. However, fixed and rotating devices are required to control antenna deformation through mechanical rotation, which is limited by cost and application. Zainud-Deen et al. [20, 21] have done a lot of work in reconfigurable antennas and antenna arrays.

It can be seen that research on plasma antennas has made certain progress. However, there are still problems such as fast reconstruction of antenna polarization and improvement of antenna gain that need to be addressed. In addition, the gain of the traditional single-ended plasma antenna is not high when the plasma vibrator is short. Therefore, a plasma antenna array is designed by combining a plasma vibrator, a cross array, and self-made regulating circuits among the vibrators. The vibrator length and plasma density can be adjusted electronically. The polarization performance of the antenna can be realized quickly and conveniently by changing the number of working vibrators and the phase difference between the adjacent vibrators.

The remainder of this paper is organized as follows. In Section 2, the design of the antenna array is discussed. Section 3 illustrates antenna reconstruction and the basic design principle of the antenna array. Section 4 demonstrates the antenna performance from the perspective of simulation and empirical test methods.

2. Construction of the Plasma Antenna Array

2.1. Design and Structure of the Plasma Antenna. The design details of the proposed plasma antenna array are shown in Figure 1. Both the frequency band and reconstruction can be determined by the antenna's substructure. The main body of the antenna array is composed of 4 vibrators (plasma column), a fixed device, regulating circuits, and a plasma exciting device. The four vibrators of the antenna are arranged in the form of cross vibrators (the angle between the axial direction of the vibrators and the horizontal direction is 0 degrees) or inclined cross vibrators (the angles between the axial direction of the vibrators and the horizontal direction are greater than 0 degrees but less than 60 degrees) using the fixed device. The polarization characteristics of antenna array may be different under various inclination angles. The discharge tubes are filled with inert gas (neon or argon in the experiment) and a small amount of mercury. The feeding ports of vibrators 1 and 2 are connected together with a metal wire, and the same is done for vibrators 3 and 4. The metal wire connecting vibrators 1 and 2 is connected to the inner conductor of the coaxial line, and the metal wire connecting vibrators 3 and 4 is connected to the outer conductor of the coaxial line (the coaxial line is omitted in Figure 1). The plasma is excited and maintained by 40.68 MHz power supplies. The excitation electrode is an induction coil with a diameter of 2 cm and a number of turns of 6 to 8. The innovation of this study is that the dipole length of the antenna array can be changed by adjusting the discharge power and the regulating circuits. In the regulation circuit system, several coupling rings are connected at different positions of the discharge tube. The coupling rings are connected to the controlling switches by the coaxial line. Taking switch 1 as an example, when switch 1 is closed, coupling ring 1 is connected to the regulation circuit, and the plasma length remains unchanged after the power is continuously increased. By changing the switch working state of different coupling rings, not only the antenna length can be changed, but also a high electron density can be maintained. In traditional single-ended excitation, the plasma density varies significantly along the axial direction. Moreover, as the discharge power increases, the antenna length becomes longer, until the plasma completely fills the discharge tube. As a result, when the length of the antenna oscillator is short, the antenna gain is low. The regulating circuit solves the problem that the gain of the traditional surface wave plasma antenna is low when the plasma is not filled with the discharge tube. In the experiment, the inner and outer diameters of the discharge tube are 10 mm and 12 mm, respectively. The length of the discharge tube is 120 mm. The vibrator's (plasma column) length ranges from 50 to 118 cm by controlling the discharge power and the regulating circuits.

Two cross vibrator antennas with different structures are constructed for comparison to show the advantages of the proposed cross vibrator plasma antenna. There are four exciting electrodes, as shown in Figure 2. More specifically, sleeve antennas are wrapped around the tube ends and used to couple the signals to the discharge tubes. Note that the feeding ports of vibrators 1 and 3 are connected by a 180° phase shifting line, while feeding ports 2 and 4 are connected with another phase shifting line. For every vibrator, there is a dielectric layer between the feeding port and the shell, where the feeding port is connected to a signal source and the shell is grounded. This antenna is called a symmetrical cross vibrator antenna. The feeding ports of vibrators 1 and 2 are connected by a 3 dB power divider, and the corresponding phase difference is 90 degrees. The other cross vibrator plasma antenna array is made by us in the early stage, and the structure is from reference [19]. In the two antenna array systems, the discharge tubes are the same as those of the proposed antenna array. However, the two antenna array systems are excited by 12 kHz power supplies, and the single-ended excitation mode is adopted. The excitation mode cannot increase the plasma electron density at a fixed length because the vibrator length is changed when the power is increased. A metal antenna array with the same structure and size as the proposed plasma antenna is established for comparison of gain and reconfigurability in the experiment.

2.2. Polarization Reconfigurable Structure. The amplitude and phase can be simultaneously controlled by changing the plasma density and working state of the vibrators. The cross vibrator plasma antenna is composed of two double-arm vibrator antennas with a constant amplitude and an orthogonal feed. The reconfigurable model of the proposed cross vibrator array is shown in Figure 3(a). Vibrators 1 and 2 are connected, and vibrators 3 and 4 are the same. If the lengths of vibrators 1 and 3 are about one quarter wavelength λ shorter than those of vibrators 2 and 4, the phases of vibrators 1, 2, 3, and 4 are 0°, 90° 180°, and 270°, respectively. It should be noted that if the lengths of vibrators 1 and 3 are approximately one quarter wavelength λ longer than those of vibrators 2 and 4, the phases of vibrators 1, 2, 3, and 4 are 0°, −90°, −180°, and −270°, respectively. By controlling the length and working number of the vibrators, the polarization

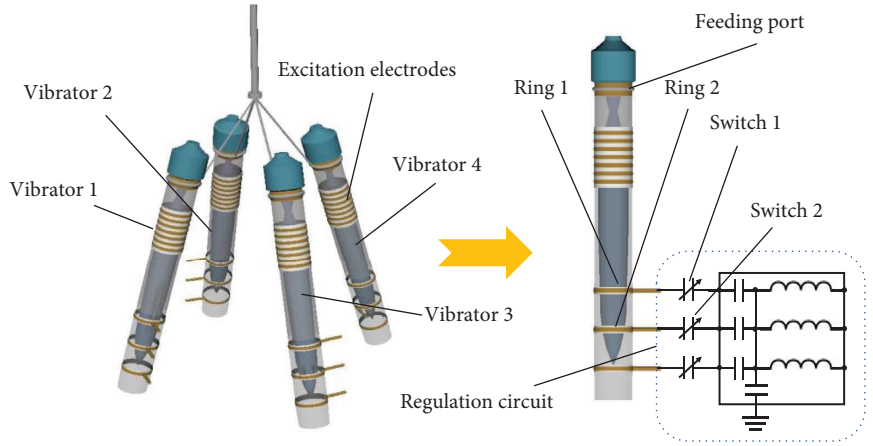

Figure 1: The schematic overview for the multi-polarized antenna array.

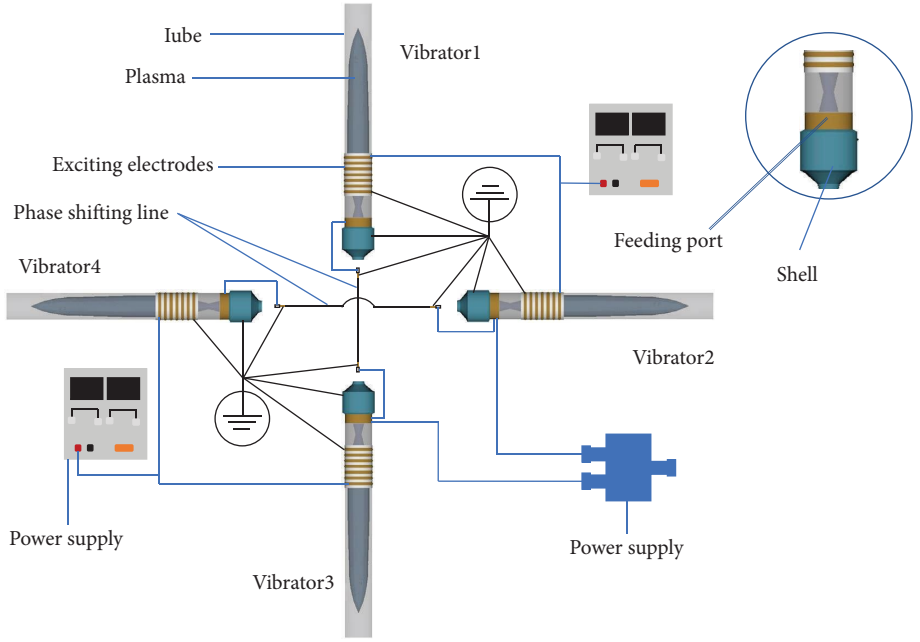

Figure 2: The schematic overview for symmetrical cross vibrator antenna.

reconfiguration containing VP, HP, LHCP, and RHCP can be easily realized. Our previous studies provide the criteria for the flexible antenna selection [17, 18]. However, the self-phase-shifting cross vibrator is a convenient yet practical method of polarization reconfiguration implementation. More specifically, polarization reconstruction can be easily realized by electronic control without mechanical device deformation, compared to the antenna structure in our previous studies [16, 18]. Moreover, the feeding and beamforming networks are supplementary in the antenna system, which aims to solve the isolation and matching problems of feeding and beamforming networks [19].

For each of the two double-arm vibrator antennas, a 180-degree phase shifted transmission line is used to ensure phase difference of the four feed ports (varying by 90 degrees in turn). As shown in the symmetrical cross vibrator plasma antenna system (see Figure 3(b)), a 3 dB power divider is utilized to provide two signals with equal amplitude and orthogonal phase difference. One of the power divider output ports is connected to the feed end of vibrator 1, and the other is connected to vibrator 2. The phase difference of oscillator 3 behind oscillator 1 is 180°, and this rule is applicable to the phase difference between vibrators 4 and 2 (see Figure 3(b)). Owing to the quadrature characteristics of the power divider, the phases of vibrators 1, 2, 3, and 4 are set to 0°, 90°, 180°, and 270°, respectively. In this manner, we can easily achieve the CP. The RHCP and LHCP can be transformed into each other by changing the phase difference between the two ports of the power divider. The proposed antenna can efficiently control the plasma parameters and the vibrator working status.

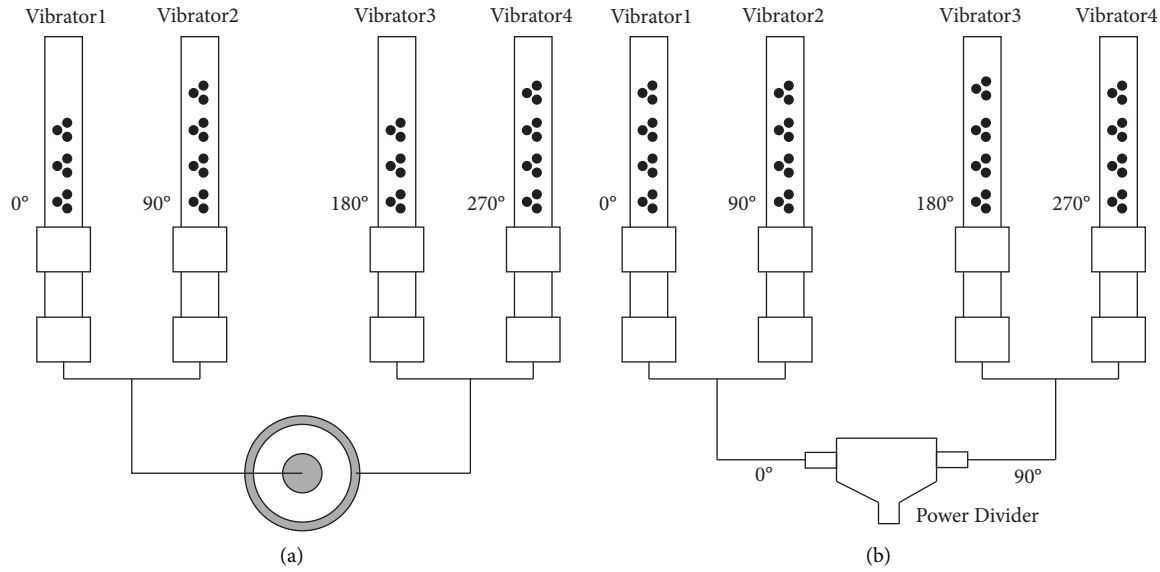

Figure 3: The reconfigurable model of the cross vibrator plasma antenna: (a) self-phase-shifting cross vibrator; (b) cross vibrator antenna with power divider.

3. Basic Principle

Conventional circularly polarized plasma and metal antennas can only radiate RHCP or LHCP signals. For instance, the polarization of the helical antenna is determined by the winding direction of the helix [18]. The vibrator antenna array system contains four vibrators, and the plasma medium for each vibrator is considered as a good conductor owing to its ionization capability. When an excitation signal propagates along the discharge tube, the maximum value of the EM field in an ideal space environment exponentially decreases in the radial direction of the column. The complex permittivity of the excited plasma can be expressed using the following equation [17, 19]:

$$\varepsilon_r = 1 - \frac{\omega_{\text{pe}}^2}{\omega\left(\omega - j\upsilon_{\text{en}}\right)}, \tag{1}$$

where υ_{en} is the plasma collision frequency, ω is the angular frequency of the EM wave, and ω_{pe} is the angular frequency of the plasma, and the plasma conductivity is obtained with the following equation:

$$\sigma = \frac{e^2 n_e}{m_e}\left(\frac{\upsilon_{\text{en}}}{\omega^2 + \upsilon_{\text{en}}^2} - j\frac{\omega}{\omega^2 + \upsilon_{\text{en}}^2}\right), \tag{2}$$

where n_e is electron density related to the collision cross section and the electron velocity. Besides, the plasma vibrator is similar to a metal vibrator when ω_{pe} is significantly larger than ω. The plasma column is produced and maintained by the kHz, MHz, or GHz input discharge signals. m_e is the mass of an electron. It is found that plasma conductivity is affected by the electron density at a fixed collision frequency [22]. Besides, the plasma vibrator is similar to a metal vibrator when ω_{pe} is significantly larger than ω. The plasma column is produced and maintained by the kHz, MHz, or GHz input discharge signals. The electrical current distribution of the plasma antenna can be quantified by considering the signal wavenumber, and the corresponding formulas can be found in (3)–(5) [18].

$$k_{r\perp} = k^2 - \frac{\varepsilon_r \omega^2}{c_0^2}, \tag{3}$$

$$k_{d\perp} = k^2 - \frac{\varepsilon_d \omega^2}{c_0^2}, \tag{4}$$

$$\varepsilon_d k_{r\perp} I_0\left(k_{r\perp} a\right) K_1 + \varepsilon_r k_{d\perp} I_1\left(k_{r\perp} a\right) K_0\left(k_{d\perp} a\right) = 0, \tag{5}$$

where c_0 is the light speed in vacuum and ε_r and ε_d are the relative permittivities in and around the vibrator, respectively. $I_n(\cdot)$ and $K_n(\cdot)$ are the first and second modified Bessel functions of integer order n. The current distribution $I(z)$ along the plasma vibrator can be reformulated as

$$I(z) = I_0 \times \left[e^{-j\int_0^z k_r \mathrm{d}z} \times e^{-\int_0^z k_j \mathrm{d}z} - e^{-j\left(2\int_0^l k_r \mathrm{d}z - \int_0^z k_r \mathrm{d}z\right)} \times e^{-\left(2\int_0^l k_j \mathrm{d}z - \int_0^z k_j \mathrm{d}z\right)}\right], \tag{6}$$

where I_0 is the current magnitude, l is the antenna length, z is the axial distance from the bottom of the vibrator, and k_r and k_j are the real and imaginary parts of the wavenumber $k(z)$, respectively. Antenna theory indicates that the far-field radiation can be expressed as

$$F(\theta) = \left| \frac{\sin\theta}{I_{\max}} \int_{-l}^{l} I(z) \exp[jk(z)z\cos(\theta)]\mathrm{d}z \right|, \tag{7}$$

where $I_{\max}$ is the maximum current and z is the distance along the axial direction of the plasma column. The CP antenna can easily fulfil the polarization matching task. A cross vibrator structure with two perpendicular dipole antennas is established. The relative amplitude and phase of each vibrator can be modified by adjusting the plasma parameters, as shown in Figures 1 and 2. The circular polarization signal is generated by the rotation of a linear vector field. Reference [19] shows the phase relationship between the horizontal polarization (HP) and vertical polarization (VP) elements as follows:

$$\begin{aligned} \partial_x &= -\tan\frac{|B_x|}{G_x} < 0, \\ \partial_y &= -\tan\frac{|B_y|}{G_y} > 0, \end{aligned} \tag{8}$$

where ∂_x and ∂_y represent the conductance in x- and y-directions, $\partial = \partial_x - \partial_y = -90^\circ$, and the polarization mode is RHCP. Besides, the polarization mode is LHCP when $\partial = \partial_x - \partial_y = 90^\circ$. B_x and B_y represent the susceptance in x- and y-directions, respectively [19].

4. Parametric Study and Performance Analysis

We conduct a series of experiments to investigate antenna performance by testing parameter setting sensitivity. Some additional parameters are determined using the simulation results. The fabricated cross vibrator plasma antenna array is shown in Figure 4, which contains four fluorescent tubes filled with argon and mercury. The length of the fluorescent tube length is 120 mm, which can be modified by adjusting the discharge state. We tested the performance of two other types of cross antennas, which can be mutually transformed by changing the feeding model and the discharge state.

4.1. Plasma Parameter. The tubes (which are custom designed) are filled with Ar and Hg at about 50 Pa. In our previous study, DC, 50 Hz AC, 5–40 kHz AC, 1–40.68 MHz AC, and 2.45 GHz AC power supplies are used to produce plasma vibrators and antenna arrays [16–19]. The electron temperature and density are measured using an optical spectrometer and a Langmuir double probe system, as shown in Figure 5. Table 1 shows the range of plasma electron temperature and density under different discharge powers. It is clear that the electron densities of plasma driven by 40.68 MHz AC and 2.45 GHz AC power supplies are higher, and the highest value reaches $10^{19}\,\mathrm{m}^{-3}$. The gain of the antennas driven by 40.68 MHz AC and 2.45 GHz AC power supplies is higher than that driven by other sources. In our experiment, it is difficult for the microwave power supply to generate the four proposed vibrators because of too large volume and power of the power supplies. Additional multiple MHz excitation sources are required to generate an antenna array. The DC and 50 (or 60) Hz AC sources are not employed because of their very large noise [23, 24].

The electron temperature, density, and starting time of the plasma vibrator at different discharge powers are systematically measured in our study. The light-electricity time difference method is used to measure the starting time (or switch-on time), which reflects the polarization reconstructed speed and the established velocity of the antenna system. The results are shown in Table 2. The values are obtained by averaging multiple measurements. Switch 1 connected to metal ring 1 (70 cm from the end) is closed, and it is observed that when the plasma column (vibrator) does not reach the position of coupling ring 1, the length of the plasma column increases with an increase in the discharge power. When the vibrator length reached 70 cm, owing to the effect of the control circuit, the discharge power continued to increase, and the antenna length remained unchanged at 70 cm, while the electron density increased. The experimental results suggest the plasma switch-on time decreases from about 300 to 60 μs, and it indicates that the antenna can achieve rapid reconstruction.

4.2. Configurable Results of Frequency Band. The vibrator length and plasma parameters can be changed by adjusting the discharge power. Thus, the antenna array can easily reconstruct the frequency band. The voltage standing wave ratio (VSWR) can be measured directly by the network analyzer (Keysight N9918A, 9 kHz–14 GHz). The characteristic impedance of the transmission line is equal to the 50 Ω output impedance of the network analyzer. Following the rules in [17, 25], the input impedance of the antenna feeding port can be analyzed by switching on/off the antenna array vibrator. Therefore, the relationship between the input impedance and VSWR can be expressed as (10).

$$Z_{\mathrm{in}}(z') = \frac{U(z')}{I(z')} = Z_0 \frac{1+\Gamma(z')}{1-\Gamma(z')}, \tag{9}$$

$$\mathrm{VSWR} = \frac{1+|\Gamma(z')|}{1-|\Gamma(z')|}, \tag{10}$$

where Z_0 is the characteristic impedance of transmission line. We test two types of cross vibrator plasma antennas: symmetrical cross vibrator antenna with power divider and the proposed plasma antenna array. The discharge power is chosen from 0 to 50 W, and the length and diameter of each vibrator ranged from 40 to 118 cm and 12 mm, respectively. The experimental platform is ANSYS HFSS 2021 based on the finite element method (FEM). The two antenna systems

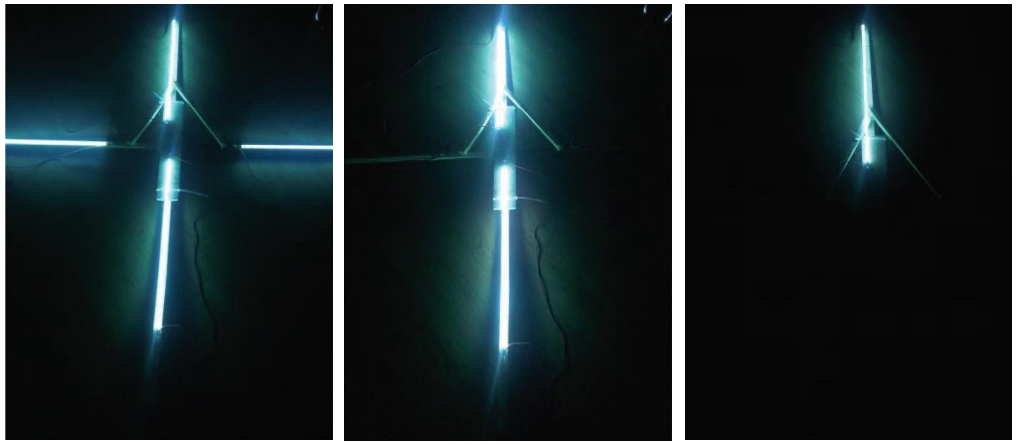

Figure 4: Photographs of the designed cross vibrator plasma antenna array (the antenna array and the symmetrical cross vibrator can be converted to each other by changing feeding status).

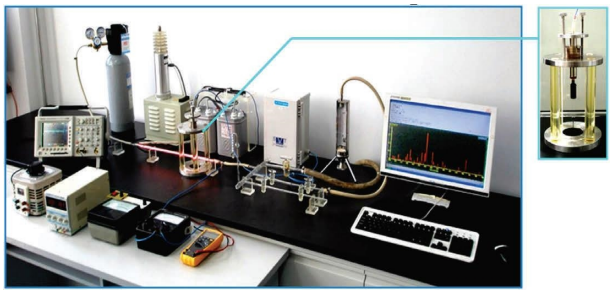

Figure 5: Measurement facility for electron temperature, density, and the switch-on time.

Table 1: Range of electron temperature and density of plasma vibrator generated by different power supplies.

Sources	DC	50 Hz	5–40 kHz	1–40.68 MHz	2.45 GHz
Temperature (eV)	1-2	1–3	1–3	1–4	1–5
Density (m^{-3})	10^{14}–10^{16}	10^{14}–10^{16}	10^{14}–10^{17}	10^{14}–10^{18}	10^{15}–10^{19}

Table 2: Measurement results of some parameters of plasma vibrator driven by 40.68 MHz power supplies when switch 1 is closed.

Power (W)	1.0	5.0	12.0	25.0	35.0
Density (m^{-3})	3×10^{14}	10^{16}	7.5×10^{16}	4.0×10^{17}	8.0×10^{17}
Starting time (μs)	280	176	130	98	64
Vibrator length (cm)	30	57	70	70	70

in Figure 6 are set based on the schematic settings following the rule in [26]. The simulation model was established by introducing plasma conductivity and permittivity from functions (1) and (2). The axial distribution of electron density in plasma vibrator is inhomogeneous. In the simulation model, the vibrator is divided into ten equal zones, and the electron density is amplified to the maximum magnitude in terms of excitation, which shows a decreasing tendency along the vibrator length [26–28].

In addition, the Langmuir double probes are embedded along the discharge tube to estimate the electron density distribution of the vibrator at different discharge powers as shown in Figure 5. When the discharge power increases to a certain value, the axial distribution of electron density can be seen as uniform. The model of the cross vibrator antenna array is shown in Figure 6(a), and the length difference between adjacent vibrators is about one-fourth to that of wavelength λ. The model of symmetrical cross vibrator antenna is shown in Figure 6(b). The experimental and simulated results for the VSWR are shown in Figure 7. Note that the tube is filled with Ar and Hg, and the gas pressure is approximately 50 Pa. The discharge power is 12 W, and the discharge frequency is 40.68 MHz. The electron temperature T_e is close to 2 eV. The electron density ranged from 10^{16} to 10^{18} m^{-3}, and the corresponding plasma angular frequency ω_{pe} varied from 6 to 90 GHz. We can obtain different vibrator lengths by changing the power inputs, and thus the frequency band can be adjusted as well. The empirical

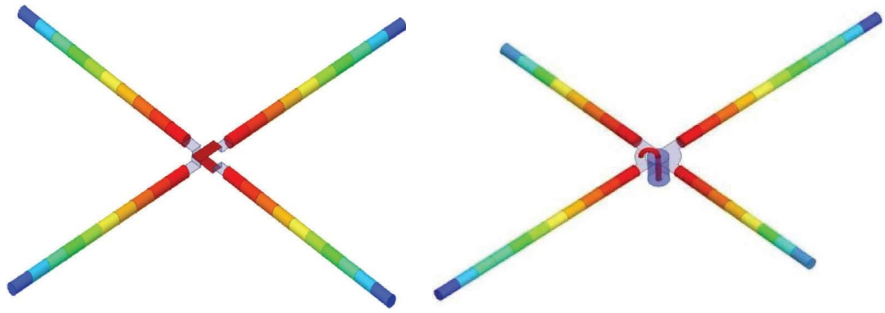

(a) (b)

FIGURE 6: Schematic overview of simulated antenna setups for the two types of cross vibrator plasma antennas. (a) Cross vibrator antenna array. (b) Symmetrical cross vibrator antenna.

frequency is close to the simulated data. It is worth mentioning that the empirical impedance bandwidth obtained is larger than the simulated one. The main reason may be that the axial distribution of election density is supposed to be uniform actually, which is in disorder during the experiments. Besides, when ω_{pe} is small, the loss of EM by plasma is a little large. Moreover, perhaps due to the unstable discharge state, when the discharge power is low, the experimental results of VSWR fluctuate significantly compared to the simulation results. It also can be seen that adjusting the antenna length can alter the operating frequency of the antenna.

4.3. Pattern Results and Discussion. In the proposed cross vibrator plasma antenna system, the pattern can be reconstructed by changing the length and the working mode of the vibrators. An anechoic chamber is used; due to the large size of the plasma antenna system, multiple receiving antennas are arranged around the antenna array. The distance between receiving antennas and the center of the antenna system is 20 m. The gain in each direction is obtained by averaging multiple measurements. The antenna length and switch status can be modified by varying the input power, the plasma parameters, and other factors. Radiation pattern reconfiguration is an important parameter for an antenna, and it includes multiple characteristics such as gain and polarization. The results of the normalized radiation pattern in the vertical plane with vibrator 1 switched on or vibrators 1 and 3 switched on are shown in Figure 8. This is because the patterns when opening vibrator 1 is nearly the same as those when opening vibrators 1 and 3 simultaneously. The working frequency is fixed at 200 MHz. In the experiment, vibrator lengths are 80 cm and 110 cm, respectively, and the corresponding discharge powers are 18 W and 28 W. The parameters for the column vibrator were set for simulation as follows: plasma angular frequency ω_{pe}, 15 to 45 GHz; length of plasma column (vibrator), 80 to 110 cm; collision frequency ν_m, 0; and the signal frequency ranges from 100 to 400 MHz. As shown in Figure 8, the shape of the radiation pattern can be changed by modifying the antenna length. For Figures 8(a) and 8(b), the simulated and empirical results are similar. When the length of the oscillator reaches 1.1 m, there is a slight difference between the experimental and simulation results, especially in the direction of the pattern and the beam width. It may be because of the errors in the distance between different receiving antennas and transmitting antennas during the experiment. The pattern results for the antenna are shown in Figure 9. At this time, the switch of coupling ring 2 (80 cm from the feeding end of the tube) is closed and the discharge powers are set at 28 W and 40 W, respectively. Therefore, the vibrator length is fixed at 80 cm. The results suggest that the shape of the radiation pattern cannot be significantly modified by changing ω_{pe}. However, the gain varies greatly.

4.4. Results of Polarization Reconfiguration. Polarization conversion of the antenna is very important for both the symmetrical cross vibrator system and the cross vibrator antenna system. Figure 10 shows the conversion methods between HP antenna, VP antenna, and CP antenna in the symmetrical cross vibrator system. The antenna is a combination of VP and HP. The conversion of HP, VP, and CP can be achieved by changing the number of activated vibrators and the discharge power. As indicated in Figure 10, the antenna is characterized by VP when switching on the vertical elements (Figure 10(a)). Figure 10(b) shows that the antenna is characterized by HP by switching on the horizontal vibrator(s). The horizontal pattern of the HP antenna is shown in Figure 11 and is similar to that in Figure 9(a). However, the maximum directional ratio of the directional pattern is biased upward, possibly because of the reflection of the earth. Moreover, the CP may be fulfilled by switching the vibrators in the antenna system. We test the two types of cross vibrator plasma antennas: a cross vibrator antenna array and symmetrical cross vibrator antenna with power divider. The discharge power is from 0 to 50 W, and each vibrator has a length of 40 to 118 cm and a diameter of 10 mm. The estimated plasma parameters are converted to conductivity and permittivity values.

We compare the polarization performance of two plasma antenna arrays (the proposed plasma antenna and the symmetrical cross vibrator antenna) at different working frequencies. Figure 12 shows the normalized polarization patterns of the two antenna systems with all the four vibrators switched on. The working frequency is 200 MHz. In the antenna array system, the lengths of the long vibrators (1,

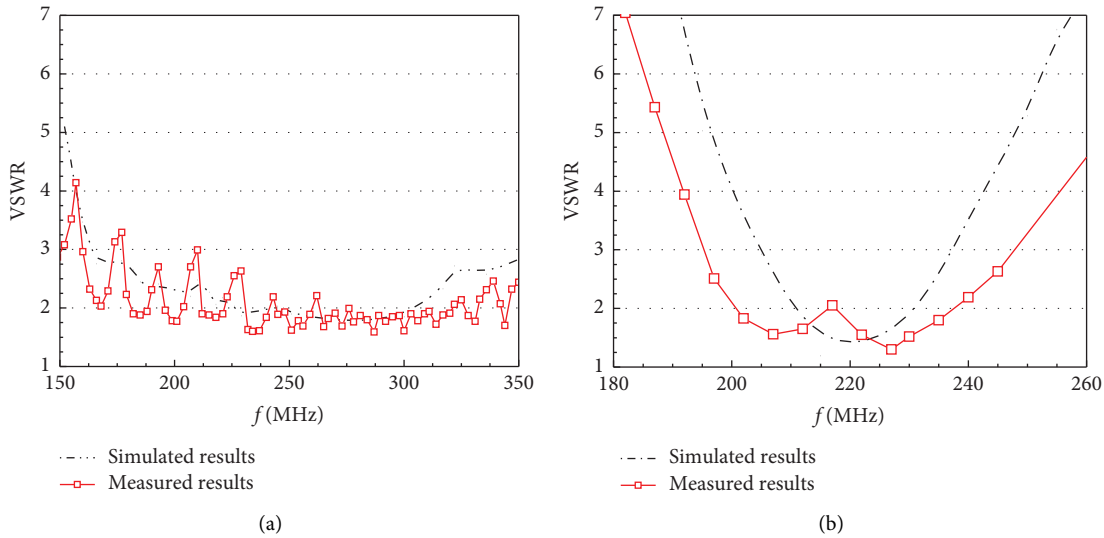

Figure 7: The measured and simulated results of vibrator VSWR. (a) Vibrator length: 57 cm, discharge power: 5 W. (b) Vibrator length: 70 cm, discharge power: 25 W.

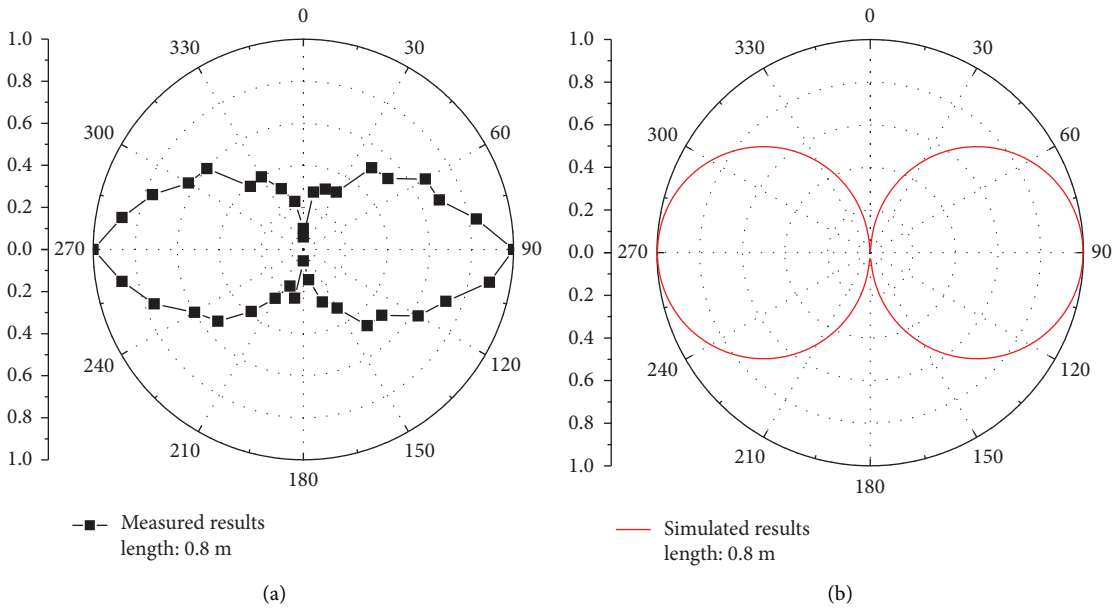

Figure 8: Continued.

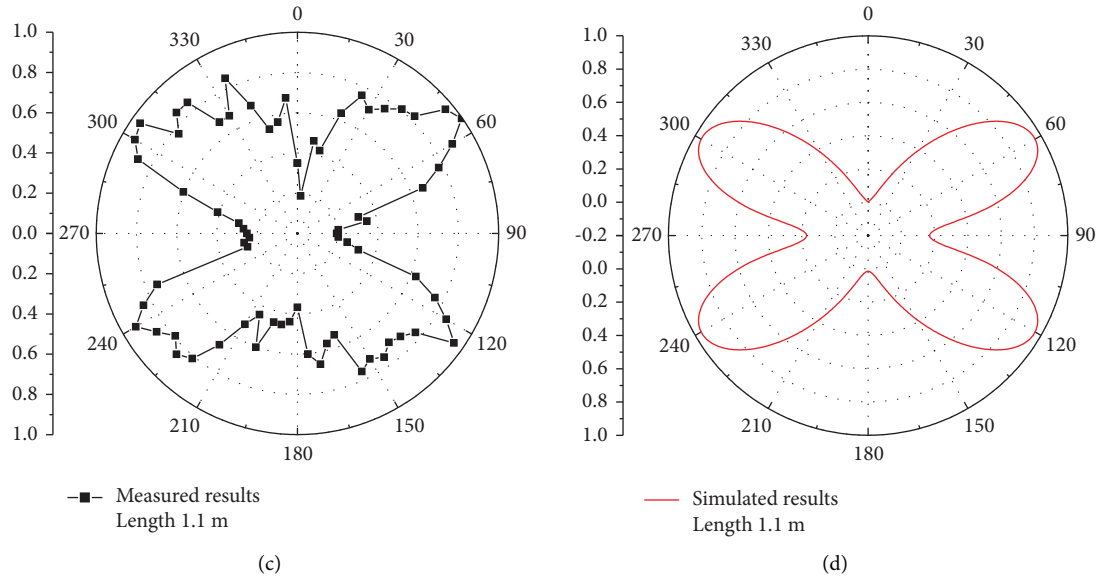

Figure 8: Radiation pattern of the antenna array system with one vibrator under working conditions. (a) Empirical results with a length of 80 cm. (b) Simulation results with a length of 80 cm. (c) Empirical results with a length of 110 cm. (d) Simulation results with a length of 110 cm.

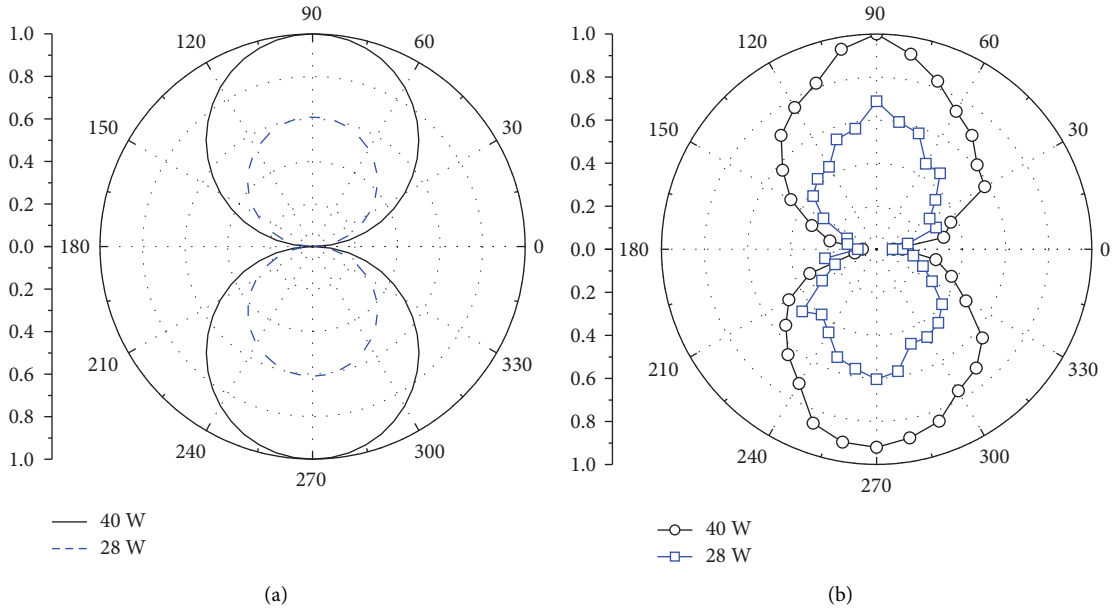

Figure 9: Radiation pattern of the antenna array system with a fixed length of 1 m and different discharge powers: (a) simulation results and (b) experimental results.

3) and short vibrators (2, 4) are 105 and 85 cm, respectively. Both the discharge powers of the long and short vibrators are 28 and 20 W, respectively. The discharge power and length of each vibrator of the comparison antenna are 28 W and 105 cm, respectively. As shown in Figure 12(a), the gain of the LHCP pattern is approximately 40% to 50% of that of the RHCP pattern. Meanwhile, from Figure 12(b), the gain of the LHCP pattern is approximately 50% to 60% of that of the RHCP pattern. The two antennas exhibit certain RHCP characteristics. In addition, compared with the comparison antenna, the simulation results are closer to the experimental results because the axial distribution of the plasma electron density in the comparison antenna is uneven. Figure 13 shows the normalized polarization patterns of the two antenna systems with a working frequency of 300 MHz. The experimental conditions in Figure 13(a) are as follows: lengths of long and short vibrators, 85 cm and 70 cm, respectively; discharge powers of long and short vibrators, 35 W. The experimental conditions in Figure 13(b) are the same as those in Figure 12(b). From Figure 13(a), the gain of

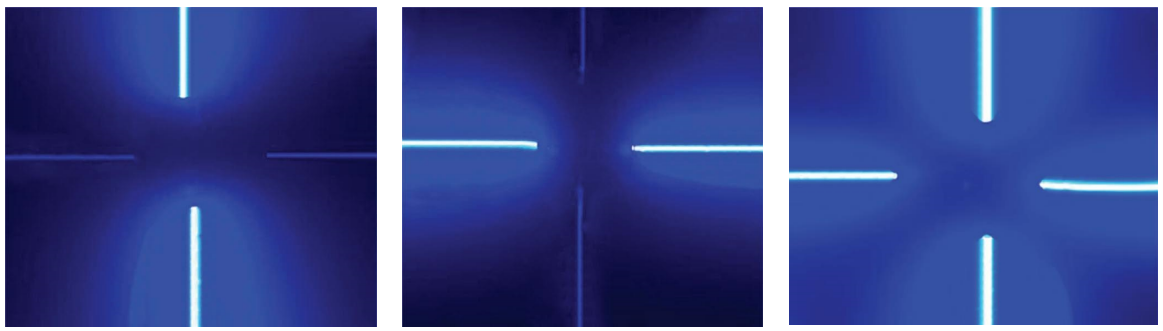

Figure 10: Different polarization for the vibrator plasma antenna: (a) VP antenna, (b) HP antenna, and (c) CP antenna.

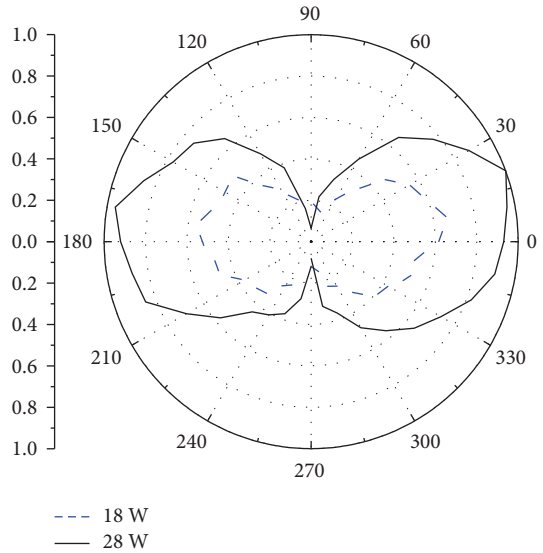

Figure 11: Empirical H-plane patterns of the antenna system with horizontal vibrators in working mode.

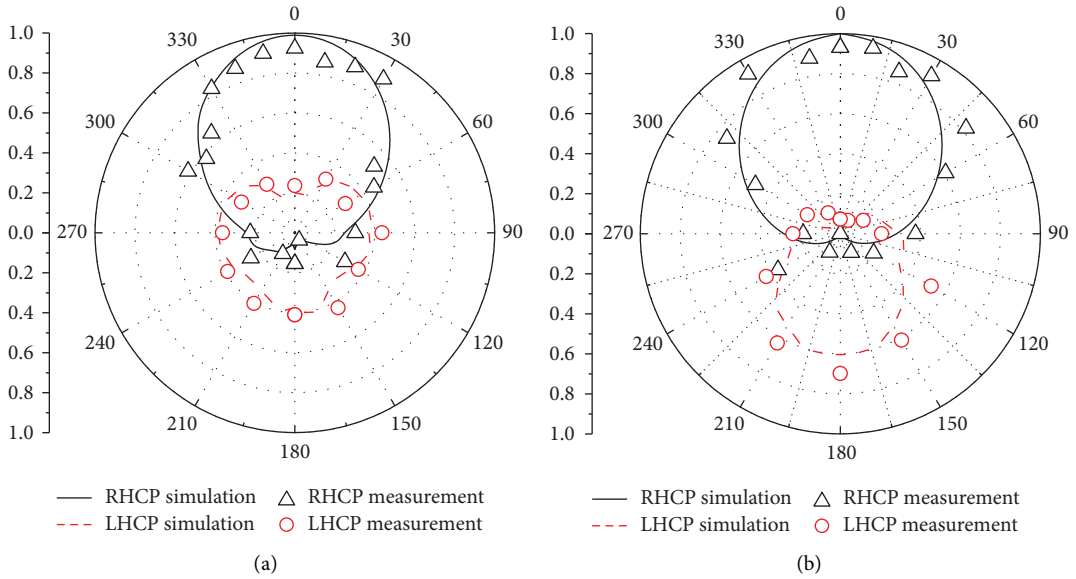

Figure 12: The polarization patterns of the proposed antenna array MHz (a) and the comparison plasma antenna (b) at a working frequency of 200 MHz.

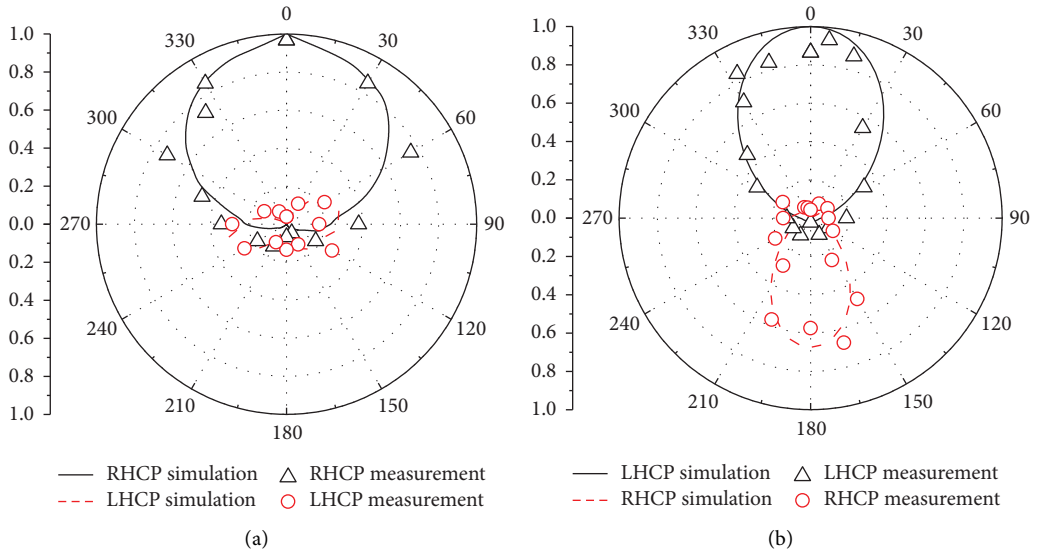

Figure 13: Comparison of polarization patterns between the proposed antenna array (a) and comparison plasma antenna (b) with a working frequency of 300 MHz.

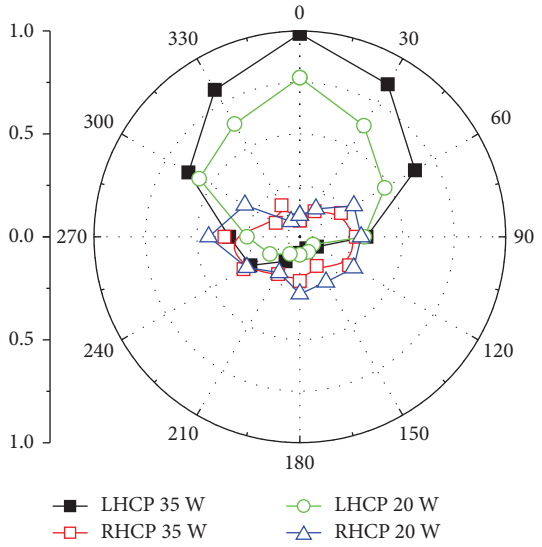

Figure 14: LHCP obtained by self-phase-shifting cross vibrator plasma antenna at different discharge powers.

the LHCP pattern is approximately 20% of that of the RHCP pattern. In this way, the cross vibrator plasma antenna array shows satisfied RHCP characteristics in a wide range of angles. This indicates that increasing the plasma electron density and changing the vibrator length can optimize the polarization performance of the antenna. However, as shown in Figure 13(b), the gain of the LHCP pattern is above 60% of that of the RHCP pattern. It is difficult to rapidly change the polarization performance of an antenna.

The LHCP is fulfilled by making vibrators 2 and 4 long vibrators (length: 85 cm) and vibrators 1 and 3 short vibrators (length: 70 cm). The LHCP patterns of the cross vibrator array are shown in Figure 14. Two types of discharge powers are applied to four vibrators, 35 W and 20 W. It can be observed that the cross vibrator plasma antenna array presented LHCP characteristics with a working frequency of 300 MHz. Besides, the polarization performance of the antenna deteriorates as the discharge power decreases. The proposed cross vibrator antenna array integrated the characteristics of VP, HP, RHCP, and LHCP. We compare the gains of plasma antenna with those of metal antenna of the same shape, as shown in Figure 15. For the plasma antenna, there are two cases. (1) The discharge powers of vibrators 1 (3) and 2 (4) are adjusted at 18.4 W and 6.4 W, respectively. The corresponding lengths of 1 (3) and 2 (4) are 70 cm and 56 cm. (2) Both the discharge powers of vibrators 1 (3) and 2 (4) are adjusted at 18.4 W, and the lengths of the long and short vibrators remain unchanged. It can be seen that when the discharge power is increased, the antenna gain also increases. The gain of the antenna is close to that of the

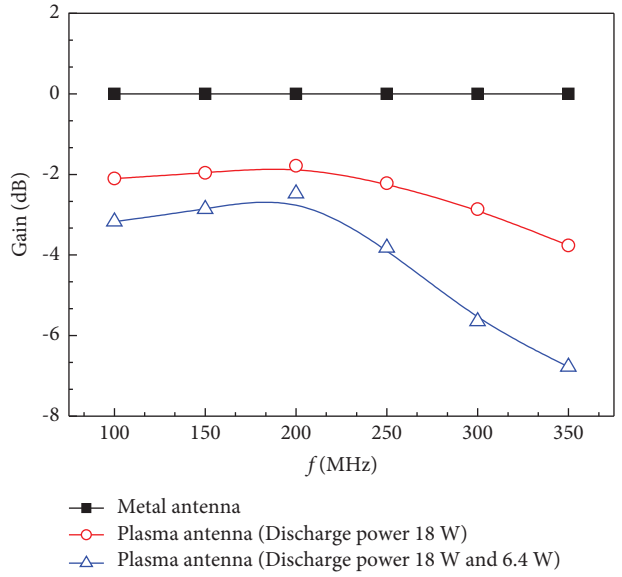

Figure 15: Gain comparison between plasma antenna and metal antenna.

Table 3: Comparison with similar works.

Antenna type	Polarization type	Polarization reconstruction	Gain (150–200 MHz)	Reconstruction time
Proposed plasma antenna array	CP, LP	Yes	−2.5 to −1.6 dBi	20–70 microseconds
Axial mode helix plasma antenna	CP	No	−4.8 to −3.5 dBi	—
Normal mode helix plasma antenna	LP	No	−4.2 to −3.2 dBi	—
Flexible plasma antenna	CP, LP	Yes	−4 to −2.7 dBi	1 millisecond
Cross vibrator plasma antenna	CP, LP	Yes	−4 to −2.8 dBi	300–800 microseconds

metal antenna in a certain frequency range. When the operating frequency is greater than 350 MHz, the gain difference between the metal antenna and the plasma antenna becomes larger and larger. We have studied the polarization characteristics of antenna arrays at different inclination angles, and the directional patterns were similar. The proposed antenna array can be used in VHF communication, maritime communication, beamforming antenna [19], etc. Next, we will seek more effective ways to increase plasma electron density. Table 3 shows the performance comparison of various plasma antennas in recent years. It is clear that the antenna we recommend has certain advantages in terms of reconstruction method, reconstruction speed, gain, etc., especially in terms of reconstruction speed.

5. Conclusions

The multi-polarized plasma antenna array is designed to achieve better antenna reconstruction. Both experimental and simulation results indicate that the plasma antenna can realize impedance, pattern, and polarization reconstruction expediently. The polarization conversion between VP, HP, RHCP, and LHCP can be realized by adjusting the plasma switch status and the phase difference between adjacent vibrators. The regulating circuit allows the antenna to obtain a higher electron density while maintaining the constant vibrator length. This antenna has better polarization and gain characteristics compared to the cross vibrator plasma antenna we designed previously. Compared with the metal cross vibrator antenna, the multi-polarized array can rapidly implement the conversion between RHCP and LHCP. Next, we will find more effective ways to improve the gain.

Data Availability

Experimental data from experimental tests and electromagnetic simulations are available from the corresponding author upon request.

Conflicts of Interest

The authors declare that they have no conflicts of interest.

Acknowledgments

This study was supported by the National Key Research and Development Program of China (grant no. 2021YFC2801002) and National Natural Science Foundation of China (nos. 52201401 and 52071200).

References

[1] B. A. Belyaev, A. A. Leksikov, A. A. Leksikov, M. Serzhantov, and Y. F. Bal'va, "Nonlinear behavior of plasma antenna vibrator," *IEEE Transactions on Plasma Science*, vol. 42, no. 6, pp. 1552–1559, 2014.

[2] I. Alexeff, T. Anderson, S. Parameswaran, E. P. Pradeep, J. Hulloli, and P. Hulloli, "Experimental and theoretical results

with plasma antennas," *IEEE Transactions on Plasma Science*, vol. 34, no. 2, pp. 166–172, 2006.

[3] G. G. Borg, J. H. Harris, N. M. Martin et al., "Plasmas as antennas: theory, experiment and applications," *Physics of Plasmas*, vol. 7, no. 5, pp. 2198–2202, 2000.

[4] M. Hadaegh and F. Mohajeri, "Investigation of the resonance frequency and performance of partially plasma filled reconfigurable cylindrical TE111 mode cavity," *Physics of Plasmas*, vol. 24, pp. 53506–53511, 2017.

[5] N. Nasr, H. Mehdian, and K. Hajisharifi, "Numerical study of practical surface eigenmodes in a new applicable nested design of plasma antenna," *IEEE Antennas and Wireless Propagation Letters*, vol. 17, no. 7, pp. 1266–1270, 2018.

[6] J. P. Rayner, A. P. Whichello, and A. D. Cheetham, "Physical characteristics of plasma antennas," *IEEE Transactions on Plasma Science*, vol. 32, no. 1, pp. 269–281, 2004.

[7] A. Papadimopoulos and A. Di Iorio, "Plasma monopole antenna array," *Compel-the International Journal for Computation and Mathematics in Electrical and Electronic Engineering*, vol. 41, no. 4, pp. 1195–1204, 2022.

[8] F. Sadeghikia, M. Talafi Noghani, and M. R. Simard, "Experimental study on the surface wave driven plasma antenna," *AEU- International Journal of Electronics and Communications*, vol. 70, no. 5, pp. 652–656, 2016.

[9] M. T. Jusoh, O. Lafond, F. Colombel, and M. Himdi, "Performance and radiation patterns of A reconfigurable plasma corner-reflector antenna," *IEEE Antennas and Wireless Propagation Letters*, vol. 12, pp. 1137–1140, 2013.

[10] R. Kumar and D. Bora, "A reconfigurable plasma antenna," *Journal of Applied Physics*, vol. 107, no. 5, pp. 053303-1–053303-9, 2010.

[11] R. Kumar and D. Bora, "Experimental study of parameters of a plasma antenna," *Plasma Science and Technology*, vol. 12, no. 5, pp. 592–600, 2010.

[12] R. Kumar and D. Bora, "Wireless communication capability of a reconfigurable plasma antenna," *Journal of Applied Physics*, vol. 109, no. 6, pp. 063303-1–063303-9, 2011.

[13] H. Q. Ye, M. Gao, and C. J. Tang, "Radiation theory of the plasma antenna," *IEEE Transactions on Antennas and Propagation*, vol. 59, no. 5, pp. 1497–1502, 2011.

[14] P. Russo, G. Cerri, and E. Vecchioni, "Self-Consistent analysis of cylindrical plasma antennas," *IEEE Transactions on Antennas and Propagation*, vol. 59, no. 5, pp. 1503–1511, 2011.

[15] P. Russo, V. M. Primiani, G. Cerri, R. De Leo, and E. Vecchioni, "Experimental characterization of a surfaguide fed plasma antenna," *IEEE Transactions on Antennas and Propagation*, vol. 59, no. 2, pp. 425–433, 2011.

[16] J. Zhao, S. Wang, H. Wu, Y. Liu, Y. Chang, and X. Chen, "Flexible plasma linear antenna," *Applied Physics Letters*, vol. 110, no. 9, pp. 94108-1–94113, 2017.

[17] J. Zhao, X. Chen, S. Wang et al., "A study of the characteristics of a deformable antenna based on gas discharge," *IEEE Transactions on Antennas and Propagation*, vol. 66, no. 1, pp. 59–70, 2018.

[18] J. Zhao, Z. Sun, Y. X. Ren et al., "Experimental characteristics of 2.45 GHz microwave reconfigurable plasma antennas," *Journal of Physics D: Applied Physics*, vol. 52, no. 29, pp. 295202–295211, 2019.

[19] J. Zhao, L. Kong, X. Chen, H. Liu, and S. Wang, "Experimental study on a self-phase-shifting cross vibrator plasma antenna array," *IEEE Antennas and Wireless Propagation Letters*, vol. 21, no. 7, pp. 1343–1347, 2022.

[20] S. H. Zainud-Deen, A. M. Mabrouk, and H. A. Malhat, "Frequency tunable graphene metamaterial reflectarray," *Wireless Personal Communications*, vol. 103, no. 2, pp. 1849–1857, 2018.

[21] H. A. Malhat, A. S. Elhenawy, S. H. Zainud-Deen, and N. A. Al-Shalaby, "Planar reconfigurable plasma leaky-wave antenna with electronic beam-scanning for MIMO applications," *Wireless Personal Communications*, vol. 128, pp. 1–18, 2023.

[22] Z. Zhang, J. Zhao, X. Xu, and Y. Yin, "Experimental study on the interaction of electromagnetic waves and glow plasma," *Plasma Science and Technology*, vol. 13, no. 3, pp. 279–285, 2011.

[23] H. Ja'afar, M. T. Ali, A. N. Dagang, I. P. Ibrahim, N. A. Halili, and H. M. Zali, "Reconfigurable plasma antenna array by using fluorescent tube for wi-fi application," *Radioengineering*, vol. 25, no. 2, pp. 275–282, 2016.

[24] Z. Chen, L. Ma, and J. Wang, "Modeling of a plasma antenna with inhomogeneous distribution of electron density," *International Journal of Antennas and Propagation*, vol. 2015, Article ID 736090, 5 pages, 2015.

[25] Y. Xu, C. Cheng, and G. Zhao, "Numerical calculation of radiation pattern and impedance of column plasma," (in Chinese)," *Acta Physica Sinica*, vol. 55, no. 7, pp. 3458–3463, 2006.

[26] V. Podolsky, A. Semnani, and S. O. Macheret, "Experimental and numerical studies of a tunable plasma antenna sustained by RF power," *IEEE Transactions on Plasma Science*, vol. 48, no. 10, pp. 3524–3534, 2020.

[27] C. Wang, B. Yuan, W. Shi, and J. Mao, "Low-profile broadband plasma antenna for naval communications in VHF and UHF bands," *IEEE Transactions on Antennas and Propagation*, vol. 68, no. 6, pp. 4271–4282, 2020.

[28] C. Wang, W. Shi, B. Yuan, and J. Mao, "Pattern-steerable endfire plasma array antenna," *IEEE Transactions on Antennas and Propagation*, vol. 69, no. 10, pp. 6994–6998, 2021.